Second harmonic generation study of the antiferromagnetic NiO(001) surface

M. Nývlt,[1,2] F. Bisio,[3,2,*] and J. Kirschner[2]

[1]*Faculty of Mathematics and Physics, Institute of Physics, Charles University, Ke Karlovu 5, CZ-12116 Praha 2, Czech Republic*

[2]*Max-Planck Institut für Mikrostrukturphysik, Weinberg 2, D-06120 Halle (Saale), Germany*

[3]*CNISM, Sede Consorziata di Genova and Dipartimento di Fisica, Via Dodecaneso 33, I-16146 Genova, Italy*

(Received 9 November 2007; published 29 January 2008)

We report a second harmonic generation (SHG) investigation of the compensated antiferromagnetic NiO(001) surface. We show that bulk and surface contributions to the total SHG signal can be distinguished based on their symmetry properties and spectral dependence. We observed that the coupling of antiferromagnetic order with crystalline structure via crystal distortion effects gives rise to a clearly observable SHG signal of magnetic origin.

DOI: 10.1103/PhysRevB.77.014435 PACS number(s): 75.70.Rf, 75.50.Ee, 42.65.−k, 78.68.+m

I. INTRODUCTION

In recent years, there has been growing attention toward the study of antiferromagnetic materials.[1–8] Besides their fundamental scientific relevance, this interest is motivated by their widespread application as a fundamental ingredient of exchange-biased junctions, exploiting the contact interface between ferromagnetic (FM) and antiferromagnetic (AF) substances. In the quest for a deeper understanding of the exchange bias effect, a number of recent investigations addressed the issue of the arrangement of the AF-ordered spins in proximity of interfacial regions in contact either with vacuum[1–4] or with ferromagnetic layers.[5–8] From the experimental point of view, however, the interface-resolved investigation of AF order is a complex task, requiring both interface sensitivity and a magnetic yield in the absence of macroscopic magnetization. Thus, the number of experimental investigations of interfacial antiferromagnetism reported so far is drastically low.[1–3,8] In this context, the development of new techniques for the investigation of antiferromagnetism with interface resolution would surely extend our capabilities of accessing these elusive systems.

A few years ago, a theoretical analysis of surface second harmonic generation (SHG) from AF surfaces suggested the capability of SHG to probe the surface AF order even in the compensated case.[9,10] The lowering of surface symmetry brought about by the onset of AF ordering was predicted to give rise to additional SHG yield in correspondence to well-defined fundamental and frequency-doubled light polarizations, thus yielding a fingerprint of surface antiferromagnetism. Subsequent more refined treatments further extended the analysis of the mechanisms underlying SHG in antiferromagnets.[11,12] As it turns out, nonlinear optical techniques had already evolved as a powerful probe of AF order,[13] and as such has been developed ever since,[14,15] although attention remained focused on *bulk* properties rather than on surface effects. Recently, interface-sensitive SHG was applied to detect uncompensated spins at buried FM-AF interfaces,[7,8] taking advantage explicitly of the magnetization reversal induced by the FM layer. To the best of our knowledge, however, no SHG investigation of *surface* AF order has been reported to date.

In this paper, we report an experimental investigation of the nonlinear optical response at the second harmonic frequency generated in reflection geometry from the AF compensated NiO(001) surface. Spectroscopic excitation and symmetry analysis of the second harmonic signal have been exploited to disentangle surface and bulk signals. We correlate the surface SHG signal with structural and magnetic properties of the sample, showing that SHG yields a spin-sensitive signal via the coupling of AF order with the crystalline structure induced by crystal distortion effects, in agreement with previous experiments[14] and theoretical analysis.[12]

The NiO(001) system was chosen for this SHG study as a prototype AF substance whose magnetic and structural properties have been thoroughly investigated,[1–3,5,6,14,16–21] thus allowing to readily interpret our data in terms of established properties of the system. NiO is a charge-transfer insulator, antiferromagnetically ordered below the Néel temperature T_N=523 K. In the AF phase, Ni^{2+} ions are ferromagnetically ordered within {111} planes, with spins pointing along $(11\bar{2})$ directions.[18] Adjacent {111} planes couple antiferromagnetically.[16] Above T_N, NiO crystallizes in the cubic rocksalt structure. The onset of AF order gives rise to a small contraction of the cubic unit cell in a direction perpendicular to {111} planes,[19,20] which reduces the crystalline symmetry from cubic to trigonal. The four possible contraction directions, corresponding to the equivalent {111} planes, define the so-called *T* domains. For each *T* domain, three types of associated domains (*S* domains) can exist, with spins pointing along one of the three equivalent $(11\bar{2})$ directions. At the (001) surface, the lattice contraction gives rise to a deviation of the surface normal with respect to the paramagnetic phase of the order of 3.5′ at 300 K.[19] The surface unit cell is square in the paramagnetic state and becomes rectangular for $T < T_N$, thus accordingly lowering the surface symmetry. According to Ref. 2, the spin arrangement at the (001) surface of cleaved crystals is bulk terminated. A schematic drawing of the NiO fcc unit cell is reported in Fig. 2(a).

II. THEORY

In electric-dipole (ED) approximation, the nonlinear polarization of a medium at the second harmonic frequency 2ω can be written as

$$P_i(2\omega) = \chi^{(2)}_{ijk} E_j(\omega) E_k(\omega). \quad (1)$$

Here, $\chi^{(2)}_{ijk}$ is the second-order electrical susceptibility tensor, which, in centrosymmetric media such as NiO, is nonzero only in proximity of the surface. Thus, SHG of electric-dipole origin (ED-SHG) is a surface-sensitive probe, whose intensity and polarization dependence are functions of the $\chi^{(2)}_{ijk}$ tensor. In the AF phase, the only symmetry operations leaving the NiO(001) surface unaltered are the identity and the rotation by 180° about the normal. Accordingly, the nonlinear electrical susceptibility tensor (for a single AF domain) can be written as[9]

$$\chi^{(2)}_{ijk} = \begin{bmatrix} 0 & 0 & 0 & \boldsymbol{\chi_{xyz}} & \chi_{xzx} & 0 \\ 0 & 0 & 0 & \chi_{yyz} & \boldsymbol{\chi_{yzx}} & 0 \\ \chi_{zxx} & \chi_{zyy} & \chi_{zzz} & 0 & 0 & \boldsymbol{\chi_{zxy}} \end{bmatrix}.$$

Tensor elements on the same columns describe the SHG response to different incident polarizations ($[p_{in}\ s_{in}\ p_{in} | sp_{in}\ p_{in}\ sp_{in}]$), while elements on the same line represent contributions to different SHG output polarizations (from top to bottom, p_{out}, s_{out}, and p_{out}).[22] Boldface tensor elements arise due to the ordered spin arrangement, whereas the other elements are nonzero due to the lattice symmetry properties.

More generally, other sources of nonlinear polarization at 2ω frequency exist,[23,24] such as electric-quadrupole (EQ) or magnetic-dipole (MD) transitions, that typically lack surface sensitivity and whose contributions superimpose to the ED-SHG. However, different contributions to SHG typically exhibit different spectral dependences, as they probe surface vs bulk electronic states. In addition, their symmetry properties reflect the different symmetry properties of the respective tensors. Separation of surface and bulk SHGs can be therefore attempted based on these effects. From the point of view of the spectral dependence, bulk SHG from NiO was shown to arise mainly from a combined contribution of magnetic-dipole and electric-dipole transitions, resonantly enhanced at $2\hbar\omega$ energy whenever the primary photon energies $\hbar\omega$ was in correspondence to NiO absorptions bands.[14] Concerning the azimuthal angle dependence of SHG, we can write the total SHG from a single AF domain as

$$I_{\alpha,\beta}(\varphi) = a^{(0)}_{\alpha,\beta} + a^{(2)}_{\alpha,\beta} \cos(2\varphi - \varphi_2) + a^{(4)}_{\alpha,\beta} \cos(4\varphi - \varphi_4), \quad (2)$$

where φ is the azimuthal angle and the $\alpha(\beta)$ indices define the input and output polarizations (see Fig. 1). The relative phase angles $\varphi_{2(4)}$, which depend on α, β, are typically related to high symmetry directions of the material. The twofold anisotropic term may contain a contribution from both surface and bulk SHGs,[14,25] whereas ED-SHG is not expected to contribute a fourfold anisotropic term, which must therefore originate from bulk contributions only. No twofold anisotropic contribution is expected in the paramagnetic phase, whereas it becomes allowed for $T < T_N$ due to the AF-order-induced symmetry lowering.[25]

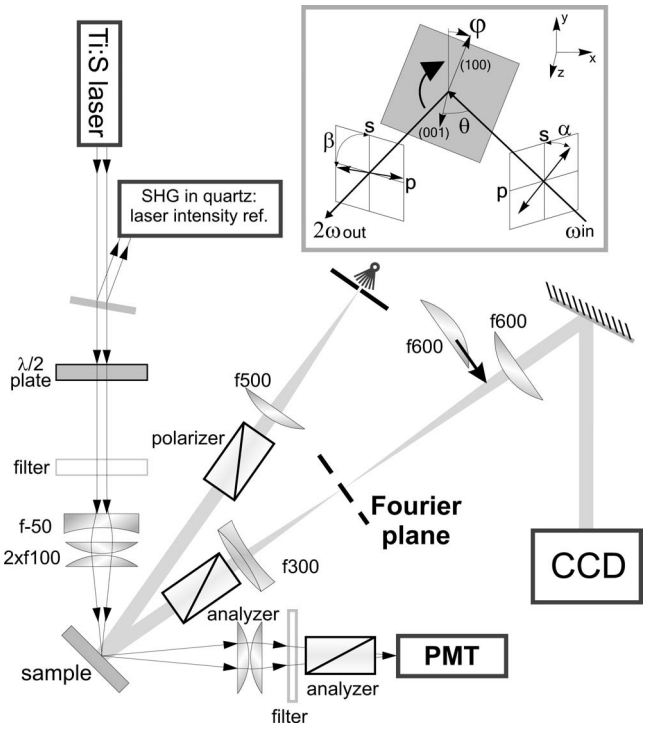

FIG. 1. Schematic diagram of the experimental apparatus employed for the linear and nonlinear optical studies of NiO(001). The inset depicts the experimental geometry for SHG measurements.

III. EXPERIMENT

A. Experimental apparatus

In Fig. 1, we report a schematic diagram of the experimental apparatus employed for the SHG measurements. The optical setup is composed of two main parts, dedicated to the linear and nonlinear optical analyses of the sample properties, respectively.

The nonlinear optical setup employs a commercial mode locked Ti:sapphire oscillator (Spectra Physics Tsunami) as radiation source, providing pulses of approximately 80 fs duration with 80 MHz repetition rate in the spectral range between 720 and 880 nm. The linearly polarized (500:1) fundamental radiation is sent through a rotatable achromatic zeroth-order half-wave-plate and focused on the surface to a spot approximately 20 μm diameter. A 3 mm thick RG 665 Schott glass filter placed before the sample removes any spurious SH radiation from optical components along the beam path. Incidence angle on the surface was set to either $\theta = 45°$ or $\theta = 7°$. Incident power was kept below 100 mW in order to avoid sample damage (this corresponds to approximately 1 nJ/pulse). Radiated SHG is analyzed by a linear polarizer and collected onto the photocathode of a photon-counting photomultiplier, whereas reflected radiation at the fundamental wavelength is rejected by a series of BG39 and BG7 optical filters. The measured SHG signal was normalized to a SHG reference measured from a quartz crystal located in a split-off branch of the beam. The SHG patterns shown in this paper were measured by recording the SHG intensity as a function of the azimuthal angle of rotation φ of the sample around its normal, measured from the (100) di-

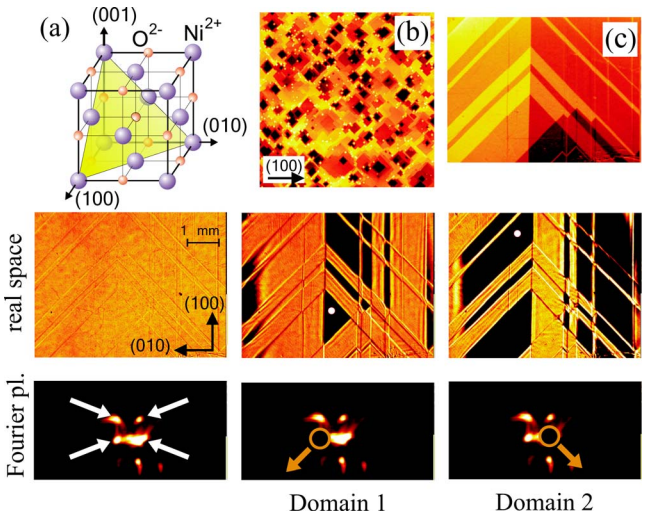

FIG. 2. (Color online) (a) Schematic drawing of the NiO fcc unit cell with the {111} plane highlighted. (b) AFM image of the NiO(001) surface after 24 h of annealing at 800 °C in O_2 atmosphere (image size 8×8 μm^2). (c) Polarized light image of the surface. Bottom part: identification of AF *T* domains by means of Fourier spatial filtration. Upper row: real-space images of the sample surface. Lower row: corresponding images of the Fourier plane. See text for details.

rection, as shown in the inset of Fig. 1. The center of rotation of the sample coincided with the laser focus on the surface within 5 μm, thus minimizing the beam walk during sample rotation. The angular precession of the surface normal during a full azimuthal rotation was less than 0.5′ for each measurement.

In the linear optical setup, parallel rays of white light generated from a point source illuminate the whole sample at 15° of incidence. The light reflected from the sample is focused by an achromatic doublet onto the Fourier plane of the lens. A movable lens system then allows either the image of the sample surface or the image of the Fourier plane to be projected onto a 16 bit resolution, cooled charge coupled device sensor, allowing the *T*-domain structure of the sample to be characterized by spatial Fourier filtration. Two linear polarizers (with extinction ratio better than 1×10^6) can be placed before and after the sample along the ray path in order to measure the linear birefringence signal from *S* domains in reflection geometry.

B. Sample characterization

Our NiO(001) sample was cleaved from a crystalline NiO rod, carefully polished and subsequently annealed for 24 h at 800 °C in oxygen atmosphere. After such treatment, greenish samples were obtained; atomic force microscopy (AFM) images [Fig. 2(b)] revealed that the surface was composed of large flat terraces extending hundreds of nanometers, bounded by steps oriented along the thermodynamically favored (110) directions. The sample was mounted on a precision goniometer and was kept at a temperature of 50 °C throughout the measurements (unless specified) in order to avoid water adsorption on the surface.

We then proceed to characterize the sample by spatial filtration techniques. In the bottom part of Fig. 2, we display optical images of the NiO(001) sample surface (in fake colors) and of its corresponding Fourier plane, measured at 350 K. In the case the surface is planar, the light intensity distribution in the Fourier plane consists of a single spot. For a NiO crystal at $T<T_N$, the light intensity distribution in the Fourier plane consists of four bright spots, arranged in a square with its sides parallel to the (100) and (010) directions, each spot corresponding to one direction of the trigonal lattice distortion. Experimentally, four bright spots, indicated by the white arrows, indeed appear in the Fourier plane (Fig. 2, bottom left).[26] Placing an opaque target in correspondence to one of the spots will prevent such area of the Fourier plane from acting as a light source concurring to form the real-space image of the surface. Thus, the surface area characterized by the direction of AF-induced distortion corresponding to the blanked spot will be imaged as black in direct space. In the bottom part of Fig. 2, we report images of the sample surface obtained after blanking various spots in the Fourier plane. The target position in the Fourier plane is indicated by the open red circle. The corresponding direction of the trigonal distortion is indicated by the red arrow. White dots on the real-space images indicate the spots chosen for SHG measurements. The domains on which SHG is performed, characterized by distortion directions parallel to the (110) or $(1\bar{1}0)$ direction, will be referred to as domains 1 and 2, respectively. Images show that *T* domains have lateral sizes comparable to 1 mm. Within each *T* domain, the birefringence signal reported in Fig. 2(c) did not show any detectable intensity variation.[27] Thus, we conclude that either the sample consists of a random arrangement of micrometric-sized *S* domains whose lateral size is below the resolution of our optical imaging apparatus or that each *T* domain consists of a single *S* domain.

IV. RESULTS

A. Surface and bulk effects

We have measured the SHG for various combinations of input and output light polarizations, chosen to provide access to different tensor elements. In the s_{in}/p_{out} geometry, ED-SHG selectively probes the χ_{zyy} tensor element which, due to its crystallographic origin, is not expected to yield a magnetic signal. In contrast, the p_{in}/s_{out} geometry probes, in ED approximation, the AF-induced $\boldsymbol{\chi_{yzx}}$ element alone, thus providing direct magnetic information, albeit at the expenses of a typically reduced yield.[21,28] The mixed $\pm sp_{in}/s_{out}$ geometry, where $+(-)sp_{in}/s_{out}$ indicates $\alpha=45°(135°)$, probes one tensor element of crystallographic origin, χ_{yyz}, and one of magnetic origin, $\boldsymbol{\chi_{yzx}}$. The SHG signal in such geometry yields information on the magnetic ordering mediated by the interference effects of the two tensor elements. The disadvantage of obtaining indirect information, however, is typically compensated by the much larger SHG signal.[28] Finally, the SHG in the s_{in}/s_{out} geometry is ED forbidden, and this geometry therefore provides a monitor of the relative importance of nonsurface effects in our experiment.

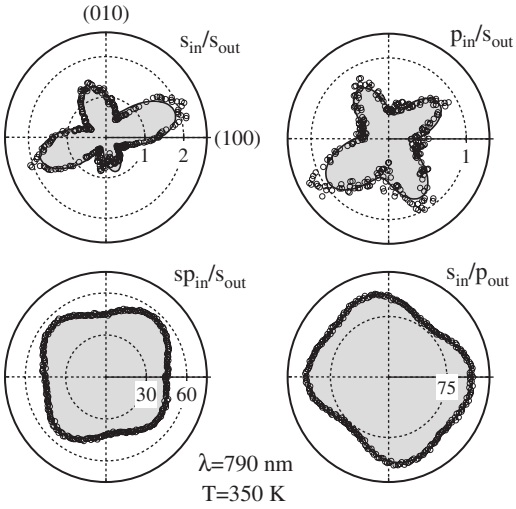

FIG. 3. Azimuthal dependence of SHG signal for different polarization geometries for fundamental wavelength λ=790 nm. Signals have been normalized to the azimuthal angle averaged s_{in}/s_{out} intensity. The angle of incidence was θ=45°; the surface temperature T=350 K. Notice the different intensity scales.

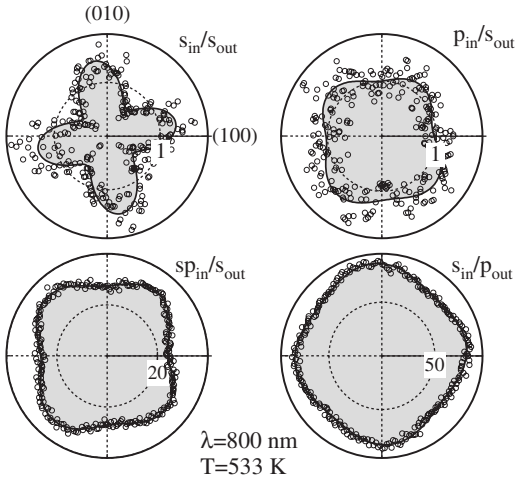

FIG. 4. Azimuthal dependence of the SHG signal for polarization geometries analogous to Fig. 3 measured at surface temperature T=533 K.

In Fig. 3, we display the SHG yield $I_{\alpha,\beta}(\varphi)$ as a function of the azimuthal angle φ measured in all the above mentioned polarization geometries at θ=45° radiation incidence angle. Sample temperature was 350 K. The SHG intensity in all geometries has been normalized to the s_{in}/s_{out} yield averaged over the azimuthal angle $\langle I_{s,s}(\varphi)\rangle$=0.97 counts/s. Data show that the SHG yield in the s_{in}/s_{out} ($I_{s,s}(\varphi)$) and p_{in}/s_{out} ($I_{p,s}(\varphi)$) geometries is extremely low, and that it exhibits a very pronounced azimuthal anisotropy. In comparison, the normalized SHG yields in the sp_{in}/s_{out} ($I_{sp,s}(\varphi)$) and s_{in}/p_{out} ($I_{s,p}(\varphi)$) geometries are larger by a factor >50, exhibiting only a rather weak azimuthal anisotropy. The anisotropic contributions for all geometries are found to be due to the superposition of twofold and fourfold symmetric contributions, in agreement with expectations.

In order to delve deeper into the mechanisms governing the 2ω radiation emission, we performed measurements for different radiation incident angles and for sample temperature $T>T_N$. Measurements performed for θ=7° incidence angle showed that the normalized SHG intensity remains identical for the p_{in}/s_{out} geometry, whereas it decreases by a factor of approximately 7 for both the sp_{in}/s_{out} and s_{in}/p_{out} polarizations. For sample temperature T=533 K$>T_N$ and θ=45°, we display the azimuthal dependence of the normalized SHG yields in Fig. 4. The azimuthally averaged s_{in}/s_{out} intensity reads $\langle I_{s,s}(\varphi)\rangle$=0.7 counts/s. The normalized yields $I_{p,s}$ and $I_{s,p}$ are comparable to the ones measured in the AF case, whereas $I_{sp,s}$ is reduced by a factor of 2. The azimuthal anisotropy in the paramagnetic phase exhibits fourfold symmetry only for all the polarization geometries, while the twofold term has disappeared.

We now focus our attention on the spectral dependence of the SHG yield. For this purpose, we first consider the p_{in}/s_{out} and s_{in}/s_{out} geometries, both characterized by extremely small signal and strong azimuthal anisotropy. The $I_{p,s}(\lambda)$ and $I_{s,s}(\lambda)$ dependences (normalized to their value at 750 nm) are reported in Fig. 5(a) (symbols), along with the wavelength dependence of the NiO linear optical absorption coefficient measured in transmission from a thinner sample (solid line). Here, λ refers to the fundamental radiation wavelength. From our data, it clearly appears that $I_{s,s}(\lambda)$ and $I_{p,s}(\lambda)$ have very similar wavelength dependence and, furthermore, that their spectral dependence closely recalls the one of the NiO optical absorption coefficient. We first conclude that the mechanism underlying SHG in the s_{in}/s_{out} and p_{in}/s_{out} geometries is analogous. Secondly, the overlap of $I_{s,s}$ and $I_{p,s}$ with the optical absorption curve suggests that s_{in}/s_{out} and p_{in}/s_{out}

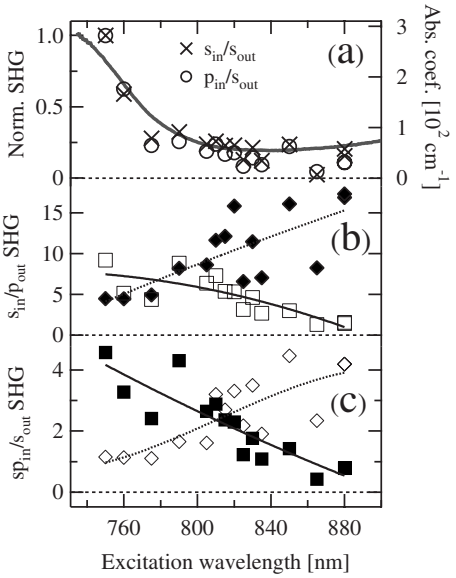

FIG. 5. (a) Spectral dependence of the NiO absorption coefficient (gray line) and of the angle integrated SHG in s_{in}/s_{out} (crosses) and p_{in}/s_{out} (open circles) geometries. (b) Spectral dependence of $a^{(2)}_{s,p}$ (full diamonds) and $a^{(4)}_{s,p}$ (open squares). (c) Spectral dependence of $a^{(2)}_{sp,s}$ (open diamonds) and $a^{(4)}_{sp,s}$ (full squares). Coefficients are defined according to Eq. (2). The lines are guides to the eye.

yields are dominated by optical transitions resonant with bulk-allowed ones, thereby lacking surface sensitivity.

At variance with the above examined geometries, the SHG $I_{sp,s}(\varphi)$ and $I_{s,p}(\varphi)$ yields are quite large, exhibit weak azimuthal anisotropy, and are strongly reduced upon reducing the incidence angle θ. The isotropic component of these yields clearly bears no information concerning the high symmetry directions of the crystal. Therefore, we focus on the spectral dependence of the anisotropic components. We obtained the $a^{(m)}_{\alpha,\beta}$ coefficients ($m=2,4$), as defined in Eq. (2), by performing best fit procedures on our data.[29] In Fig. 5(b), we report the spectral dependence of the $a^{(2)}_{s,p}$ (full diamonds) and $a^{(4)}_{s,p}$ (open squares) coefficients, whereas in Fig. 5(c), the $a^{(2)}_{sp,s}$ (open diamonds) and $a^{(4)}_{sp,s}$ (full squares) coefficients are reported. Our data show that the $\cos 4\varphi$ contributions in both s_{in}/p_{out} and sp_{in}/s_{out} geometries regularly decrease with increasing wavelength, analogously to $I_{s,s}(\lambda)$ and $I_{p,s}(\lambda)$. In contrast, the $a^{(2)}_{s,p}$ and $a^{(2)}_{sp,s}$ coefficients exhibit a different spectral dependence, as their magnitude increases with increasing wavelength, reaching the maximum in a spectral range for which fourfold contributions are negligible. Since it is well known that ED-SHG cannot contribute a $\cos 4\varphi$ term,[25] we ascribe the existence of nonzero $\cos 4\varphi$ contributions to the presence of SHG mechanisms of higher order than ED. Such mechanisms are associated with optical excitations resonant with bulk transitions and could have either EQ or MD origin. In particular, the MD mechanism cannot be excluded even though the $\cos 4\varphi$ contributions remain clearly observable also for $T>T_N$ because MD contributions do not arise from the spin magnetic moment but from the orbital angular momentum, and therefore exist even in paramagnetic state.[30] Coming to the $\cos 2\varphi$ symmetric contribution, it is known that these can contain both bulk and surface contributions.[25] The spectral dependence of the twofold component rules out the occurrence of bulk-resonant process at the energy of both the fundamental and SH radiations.[31] Since all the available experimental data show that bulk SHG is typically resonant with bulk absorption bands in NiO,[14] we have a strong indication that the $\cos 2\varphi$ components in s_{in}/p_{out} and sp_{in}/s_{out} geometries do not arise from bulk SHG contributions. Furthermore, the increase of $a^{(2)}_{s,p}$ and $a^{(2)}_{sp,s}$ with wavelength in the 720–880 nm range agrees with theoretical calculations of the wavelength dependence of the surface χ_{zyy} tensor element.[11] We therefore suggest that the twofold symmetric SHG contributions in the s_{in}/p_{out} and sp_{in}/s_{out} geometries mainly arise from surface effects. We remark that appropriate comparison of our experimental data with previous SHG studies of NiO,[14,15] which reported the absence of surface contributions in the frequency-doubled radiation, suggests that the choice of an off-normal radiation incidence geometry might prove crucial in the observation of surface SHG.

B. Symmetry analysis

In order to correlate the anisotropic $\cos 2\varphi$ SHG signal with the sample properties, we perform a symmetry analysis of the $I_{s,p}(\varphi)$ and $I_{sp,s}(\varphi)$ signals measured from different AF domains. We first focus on the s_{in}/p_{out} geometry for which,

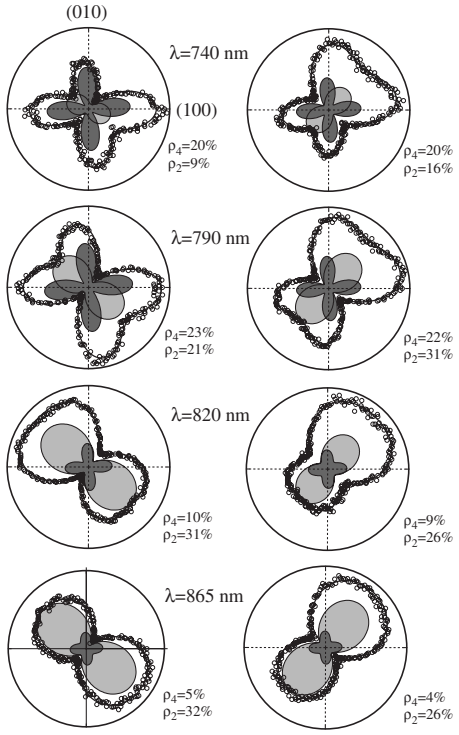

FIG. 6. Anisotropic part of $I_{s,p}$ as a function of the azimuthal angle φ measured for different fundamental wavelengths λ. Graphs report experimental data (open symbols), best fitted according to Eq. (2) (solid line), $\cos 4\varphi$ contribution (dark-gray area), and $\cos 2\varphi$ contribution (light-gray area). Not shown is the $\cos \varphi$ contribution. Left column: data measured from T domain 1. Right column: data measured from T domain 2.

in ED approximation, a single tensor element is involved in SHG. In Fig. 6, we display the anisotropic part of $I_{s,p}(\varphi)$ for different fundamental wavelengths, measured from T domain 1 (left column) and T domain 2 (right column). The $\cos 4\varphi$ and $\cos 2\varphi$ contributions are highlighted in dark and light gray, respectively, while the $\cos \varphi$ term is not reported.[29] A small isotropic offset has been added for better reading of the plots. The relative magnitude of the anisotropic terms is reported on the graphs as $\rho_m = a^{(m)}_{s,p}/a^{(0)}_{s,p}$, $m=2,4$. The data clearly show that the $\cos 4\varphi$ term gradually fades with increasing wavelength, while the twofold term gets gradually larger, becoming dominant above 800 nm. Whereas the $\cos 4\varphi$ contributions have their maximum when the projection on the surface of the radiation wave vector $\mathbf{k}_s(\lambda)$ lies along the (100) and (010) directions independently of the T domain type, the angular dependence of the $\cos 2\varphi$ anisotropic contribution exhibits a well-defined domain dependence. For T domain 1, the maximum of the twofold contribution occurs for $\mathbf{k}_s(\lambda) \| (110)$, whereas for T domain 2 the maximum occurs for the in-plane orthogonal direction $(1\bar{1}0)$.

Coming to the sp_{in}/s_{out} geometries, we have noticed that different SHG yields were obtained for $\alpha=45°$ and $\alpha=135°$ incident polarizations, even from the same T domain. In Fig. 7, we report the anisotropic part of the SHG yield for $+sp_{in}/s_{out}$ (left column) and $-sp_{in}/s_{out}$ geometries (right column) both measured from T domain 1. The $\cos 4\varphi$ term,

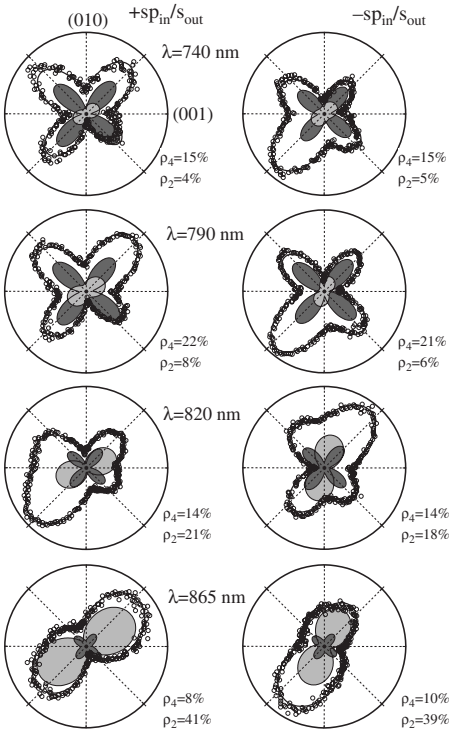

FIG. 7. Anisotropic part of $I_{\pm sp,s}$ as a function of the azimuthal angle φ measured for different fundamental wavelengths λ. Data have been measured from T domain 1. Graphs report experimental data (open symbols), best fitted according to Eq. (2) (solid line), cos 4φ contribution (dark-gray area), and cos 2φ contribution (light-gray area). Not shown is the cos φ contribution. Left column: $+sp_{in}/s_{out}$ geometry. Right column: $-sp_{in}/s_{out}$ geometry.

displayed as dark-gray area, exhibits maxima along the (110) and $(1\bar{1}0)$ directions and decreases with increasing wavelength, while the cos 2φ term correspondingly increases for both $+sp_{in}/s_{out}$ and $-sp_{in}/s_{out}$ geometries. However, data show that for the two different incident polarizations, the maxima of the cos 2φ terms occur in correspondence to different angles φ_2. These angles do not apparently correspond to any crystallographic high symmetry direction and are constant with wavelength, within experimental uncertainty. For the $+sp_{in}/s_{out}$ and $-sp_{in}/s_{out}$ cases, the wavelength-averaged φ_2 reads $\langle\varphi_2(\lambda)\rangle^{(+)}=(28\pm4)°$ and $\langle\varphi_2(\lambda)\rangle^{(-)}=(62\pm6)°$, respectively. Analogously, for T domain 2 (not shown), we have $\langle\varphi_2(\lambda)\rangle^{(+)}=(123\pm4)°$ and $\langle\varphi_2(\lambda)\rangle^{(-)}=(143\pm5)°$. For T domain 1, the cos 2φ contribution for $+sp_{in}/s_{out}$ and $-sp_{in}/s_{out}$ polarizations are therefore roughly symmetric with respect to the (110) axis, whereas for T domain 2, the corresponding twofold terms are symmetric with respect to the $(1\bar{1}0)$ direction. This suggests that the total cos 2φ contribution for each polarization is due to the superposition of two different twofold components: the first component stays constant upon rotating the incident polarization by 90° ("even" contribution) while the second component is antisymmetric with respect to the (110) axis for T domain 1 and $(1\bar{1}0)$ for T domain 2 ("odd" contribution). Since $\varphi_2(\lambda)^{+(-)}$ is experimentally constant, irrespective of the T domain, the odd and even components must have the same spectral dependence, and

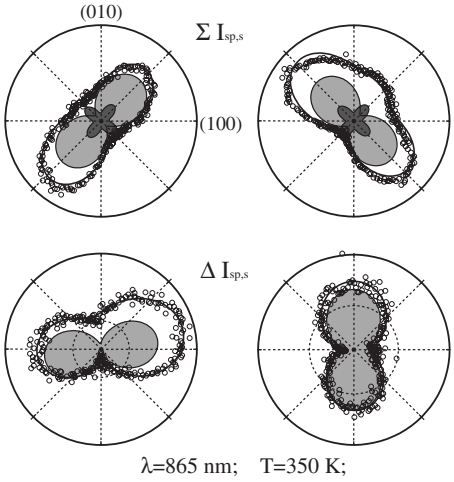

FIG. 8. Anisotropic part of $\Sigma I_{sp,s}(\varphi)$ (top) and $\Delta I_{sp,s}(\varphi)$ (bottom) as a function of the azimuthal angle φ measured for fundamental wavelength $\lambda=865$ nm. Graphs report experimental data (open symbols), best fitted according to Eq. (2) (solid line), cos 4φ contribution (dark-gray area), and cos 2φ contribution (light-gray area). Not shown is the cos φ contribution. Left column: data measured from T domain 1. Right column: data measured from T domain 2.

therefore must originate from the same mechanism. We then define the functions $\Delta I_{sp,s}(\varphi)=[I_{+sp,s}(\varphi)-I_{-sp,s}(\varphi)]$ and $\Sigma I_{sp,s}(\varphi)=[I_{+sp,s}(\varphi)+I_{-sp,s}(\varphi)]$ as the sum and difference, respectively, of the $I_{\pm sp,s}$ yields. In the $\Delta I_{sp,s}(\varphi)$ function, the even cos 2φ contribution cancels out, leaving the odd term only and vice versa for $\Sigma I_{sp,s}(\varphi)$. In Fig. 8, we report the polar plots of the $\Sigma I_{sp,s}(\varphi)$ (top) and $\Delta I_{sp,s}(\varphi)$ (bottom) signals obtained from T domain 1 (left column) and T domain 2 (right column). For T domain 1, the even cos 2φ component has its maximum for $\mathbf{k}_s(\lambda)$ parallel to the $(1\bar{1}0)$ direction, whereas the odd component is oriented to have its maximum for $\mathbf{k}(\lambda)\|(010)$, independent of wavelength. For T domain 2, the directions of the maximum are for $\mathbf{k}(\lambda)\|(110)$ and $\mathbf{k}(\lambda)\|(100)$ for the even and odd components, respectively, also independent of wavelength.

V. DISCUSSION

In the theoretical analysis of ED-SHG from AF surfaces,[9,10] symmetry arguments were employed to deduce which elements of the $\chi^{(2)}_{ijk}$ tensor became nonzero upon the onset of long range AF order. The authors suggested in which polarization combinations a contribution of such elements could be observed and analyzed, thus yielding a fingerprint of surface antiferromagnetism. The theoretical analysis was meant to apply to AF-ordered NiO crystals and included the effect of lattice distortions on the SHG.[10] Our experimental analysis therefore focused on two main issues, the possibility of observing surface-sensitive SHG from NiO and the influence of the lattice contraction along the {111} directions (referred to as {111} contraction in the following) on the SHG output.

Our data unambiguously show that the magnitude of the AF-induced $\boldsymbol{\chi}_{\mathbf{yzx}}$ is extremely small. As a consequence, the *direct* probing of this element, theoretically feasible in the p_{in}/s_{out} experimental geometry, yields a SHG signal dominated by non-ED transitions, which lack surface sensitivity. By contrast, strong indications of surface effects were found for the s_{in}/p_{out} and $\pm sp_{in}/s_{out}$ polarization combinations. The s_{in}/p_{out} geometry theoretically yields SHG signal related to the lattice symmetry, whereas the $\pm sp_{in}/s_{out}$ interestingly probes the AF-induced $\boldsymbol{\chi}_{\mathbf{yzx}}$ element, too.

In the purely crystallographic s_{in}/p_{out} geometry, we observe a clear signature of the {111} contraction effect, which manifests itself via the appearance of a $\cos 2\varphi$ contribution in the azimuthal dependence of the $I_{s,p}(\varphi)$ yield. Experimentally, we observe that the maxima of the $\cos 2\varphi$ contribution occur when the projection of the incident radiation wave vector $\mathbf{k}(\lambda)$ lies perpendicular to the direction of contraction of the surface primitive cell. The appearance of a crystallographic $\cos 2\varphi$ contribution is readily understandable on the basis of well-known symmetry effects on the azimuthal dependence of SHG signal.[25] In fact, the contraction of the bulk unit cell along the {111} (and equivalent) direction affects the surface unit cell as well, changing its shape from square at $T > T_N$ to rectangular for $T < T_N$, for which twofold symmetric signal becomes allowed. In the s_{in}/p_{out} geometry, all the symmetry operations leaving the surface unit cell unchanged do not affect the $\cos 2\varphi$ contribution. It therefore appears that these $\cos 2\varphi$ contributions are of purely crystallographic origin and bear no direct link to the magnetic ordering.

When considering the $\pm sp_{in}/s_{out}$ geometry, our analysis shows that the twofold symmetric SHG yield results from the superposition of two contributions with different symmetry properties. In ED approximation, SHG in this geometry indeed probes two tensor elements, χ_{yyz} and $\boldsymbol{\chi}_{\mathbf{yzx}}$. Despite its small magnitude, the contribution of $\boldsymbol{\chi}_{\mathbf{yzx}}$ to the total SHG yield can become observable in this mixed geometry via interference effects. We therefore ask ourselves whether the even and the odd twofold symmetric contributions to $I_{sp,s}(\varphi)$ can be identified as induced by χ_{yyz} and $\boldsymbol{\chi}_{\mathbf{yzx}}$. First of all, we notice that the even $\cos 2\varphi$ term possesses the same symmetry as the surface unit cell, analogously to the s_{in}/p_{out} geometry discussed above. This suggests that the even term is directly related to the crystallographic structure rather than to the AF order. The odd $\cos 2\varphi$ contribution, however, has its maximum for the projection of $\mathbf{k}(\lambda)$ parallel to the (010) or (100) direction for T domains 1 and 2, respectively. However, the (100) or (010) directions are *not* equivalent in a model that considers T domains only. Therefore, in order to account for the observation of (100) or (010) oriented $\cos 2\varphi$ contributions, a further symmetry lowering mechanism must be taken into account, which is necessarily related to the existence of a well-defined direction for spin alignment within each T domain. In order to determine the origin of this signal, we notice that the SHG electric field radiated due to the tensor elements χ_{yyz} has opposite signs for $\alpha = 45°$ or $\alpha = 135°$ incident polarization, whereas the field radiated due to $\boldsymbol{\chi}_{\mathbf{yzx}}$ stays invariate. Since the output SHG intensity is the square of the sum of the electric fields, it turns out that a different signal is measured for $\pm sp_{in}/s_{out}$ polarizations. Such output signal is then decomposable into odd or even contributions, as experimentally observed. The odd contribution possesses a symmetry-breaking azimuthal dependence which, according to our analysis, is the fingerprint of spin-arrangement effects on SHG. The coupling mechanism of SHG to magnetic order has to be related to the AF-order-induced lattice contraction, in analogy with the bulk SHG of Ref. 14 and with the symmetry analysis of Ref. 12. In fact, the evidence that even and odd $\cos 2\varphi$ contributions to $I_{sp,s}$ possess the same spectral dependence means that the SHG mechanism underlying their origin is identical. Since the mechanism underlying the appearance of the even $\cos 2\varphi$ contributions is connected to lattice symmetry, an analogous mechanism must be effective for the odd ones, thus leaving magnetism-induced crystal-symmetry effects (i.e., lattice contraction) as the only option. In the hypothesis, "even" terms are of surface ED origin; this must be true for "odd" terms as well because the spectral dependence of ED and non-ED contributions has been clearly shown to be different. At variance with the detailed analysis of S-domain contribution to SHG of Ref. 32, our data do not allow us, at present, to clearly correlate the spin-induced $I_{sp,s}$ signal to the occurrence of a well-defined S domain. Systematic studies from different samples exhibiting a variety of S domains are needed to delve deeper into this issue.

VI. CONCLUSION

In conclusion, we have performed a SHG investigation of AF compensated NiO(001) surface. We show that bulk and surface contributions to the total SHG signal can be distinguished based on the symmetry properties and the spectral dependence of the frequency-doubled signal. We have experimentally tested the theoretical prediction of the occurrence of nonzero elements of the second-order electrical susceptibility tensor $\chi^{(2)}_{ijk}$ in the AF magnetic phase, revealing that they possess small magnitude, which makes their observation not feasible. We observed that AF order couples with crystalline structure via magnetism-induced lattice contraction effects, in agreement with previous experiments[14] and with theoretical analysis,[12] giving rise to a clearly observable SHG signal. Our results represent a significant step forward toward the experimental investigation of surface AF order by SHG. We believe that this experiment will accordingly stimulate further work in this direction.

ACKNOWLEDGMENTS

The authors acknowledge Wolfgang Hübner and Georg Lefkidis for insightful discussion and for a critical reading of this paper and Heike Menge for preparing high-quality substrates. M.N. thanks the MSM 0021620834 research plan of the Czech Ministry of Education for financial support. F.B. acknowldeges support from the Max-Planck-Gesellschaft.

*bisio@fisica.unige.it

[1] M. Marynowski, W. Franzen, M. El-Batanouny, and V. Staemmler, Phys. Rev. B **60**, 6053 (1999).
[2] F. U. Hillebrecht, H. Ohldag, N. B. Weber, C. Bethke, U. Mick, M. Weiss, and J. Bahrdt, Phys. Rev. Lett. **86**, 3419 (2001).
[3] A. Barbier, C. Mocuta, W. Neubeck, M. Mulazzi, F. Yakhou, K. Chesnel, A. Sollier, C. Vettier, and F. de Bergevin, Phys. Rev. Lett. **93**, 257208 (2004).
[4] C. L. Gao, U. Schlickum, W. Wulfhekel, and J. Kirschner, Phys. Rev. Lett. **98**, 107203 (2007).
[5] H. Ohldag, A. Scholl, F. Nolting, S. Anders, F. U. Hillebrecht, and J. Stöhr, Phys. Rev. Lett. **86**, 2878 (2001).
[6] H. Ohldag, T. J. Regan, J. Stöhr, A. Scholl, F. Nolting, J. Lüning, C. Stamm, S. Anders, and R. L. White, Phys. Rev. Lett. **87**, 247201 (2001).
[7] L. C. Sampaio, A. Mougin, J. Ferré, P. Georges, A. Brun, H. Bernas, S. Poppe, T. Mewes, J. Fassbender, and B. Hillebrands, Europhys. Lett. **63**, 819 (2003).
[8] V. K. Valev, M. Gruyters, A. Kirilyuk, and T. Rasing, Phys. Rev. Lett. **96**, 067206 (2006).
[9] A. Dähn, W. Hübner, and K. H. Bennemann, Phys. Rev. Lett. **77**, 3929 (1996).
[10] M. Trzeciecki, A. Dähn, and W. Hübner, Phys. Rev. B **60**, 1144 (1999).
[11] G. Lefkidis and W. Hübner, Phys. Rev. Lett. **95**, 077401 (2005).
[12] G. Lefkidis and W. Hübner, Phys. Rev. B **74**, 155106 (2006).
[13] M. Fiebig, D. Fröhlich, B. B. Krichevtsov, and R. V. Pisarev, Phys. Rev. Lett. **73**, 2127 (1994).
[14] M. Fiebig, D. Fröhlich, T. Lottermoser, V. V. Pavlov, R. V. Pisarev, and H. J. Weber, Phys. Rev. Lett. **87**, 137202 (2001).
[15] N. P. Duong, T. Satoh, and M. Fiebig, Phys. Rev. Lett. **93**, 117402 (2004).
[16] W. L. Roth, Phys. Rev. **110**, 1333 (1958).
[17] H. Kondoh, J. Phys. Soc. Jpn. **18**, 1346 (1963).
[18] T. Yamada, S. Saito, and Y. Shimomura, J. Phys. Soc. Jpn. **21**, 672 (1966).
[19] L. C. Bartel and B. Morosin, Phys. Rev. B **3**, 1039 (1971).
[20] K. Nakahigashi, N. Fukuoka, and Y. Shimomura, J. Phys. Soc. Jpn. **38**, 1634 (1975).
[21] O. Ney, M. Trzeciecki, and W. Hübner, J. Phys.: Condens. Matter **17**, 7489 (2005).
[22] W. Hübner and K. H. Bennemann, Phys. Rev. B **52**, 13411 (1995).
[23] P. Guyot-Sionnest and Y. R. Shen, Phys. Rev. B **38**, 7985 (1988).
[24] J. E. Sipe, D. J. Moss, and H. M. van Driel, Phys. Rev. B **35**, 1129 (1987).
[25] D. A. Koos, V. L. Shannon, and G. L. Richmond, Phys. Rev. B **47**, 4730 (1993).
[26] Additional spots in the Fourier plane (bottom right part of pictures) are generated by a twinned section of the crystal that was accurately avoided during SHG measurements.
[27] Our apparatus possesses the necessary sensitivity to observe linear birefringence, as checked on samples of different qualities, not suitable for the present study, for which *S* domains were observed.
[28] M. Nývlt, F. Bisio, J. Franta, C. L. Gao, H. Petek, and J. Kirschner, Phys. Rev. Lett. **95**, 127201 (2005).
[29] In order to achieve good fit, an anisotropic contribution with $\cos(\varphi-\varphi_1)$ dependence, not considered in Eq. (2), has to be included. The onefold term, however, exhibits random azimuthal orientation and intensity as a function of the polarization geometry, wavelength, and *T*-domain type. It can be due neither to beam walk nor to sample-normal wobble, and we therefore ascribe it to the random sampling of defects both at the surface and in the interior of the solid due to the large optical penetration depth in NiO at the wavelengths we employ. Accordingly, this component carries no useful information about the system properties.
[30] Employing $\lambda \approx 2400$ nm excitation might elucidate the origin of the $\cos 4\varphi$ contribution, since at that frequency, only surface states exist (Ref. 12).
[31] R. Newman and R. M. Chrenko, Phys. Rev. **114**, 1507 (1959).
[32] I. Sänger, V. V. Pavlov, M. Bayer, and M. Fiebig, Phys. Rev. B **74**, 144401 (2006).